Metformin reverses oxidative stress-induced mitochondrial dysfunction in pre-osteoblasts via the EGFR/GSK-3β/calcium pathway

FANGMING CAO, KEDA YANG, SHUI QIU, JIE LI, WEN JIANG, LIN TAO and YUE ZHU

Department of Orthopedics, First Hospital of China Medical University, Shenyang, Liaoning 110001, P.R. China

Received August 30, 2022; Accepted February 15, 2023

DOI: 10.3892/ijmm.2023.5239

Abstract. Oxidative stress is one of the main causes of osteoblast apoptosis induced by post-menopausal osteoporosis. The authors previously found that metformin can reverse the loss of bone mass in post-menopausal osteoporosis. The present study aimed to further clarify the effects and mechanisms of action of metformin in post-menopausal osteoporosis under conditions of oxidative stress. Combined with an in-depth investigation using the transcriptome database, the association between oxidative stress and mitochondrial dysfunction in post-menopausal osteoporosis was confirmed. A pre-osteoblast model of oxidative stress was constructed, and the apoptotic rate following the addition of hydrogen peroxide and metformin was detected using CCK-8 assay and Annexin V-FITC/PI staining. Mitochondrial membrane potential was detected using the JC-1 dye, the intracellular calcium concentration was detected using Fluo-4 AM, the intracellular reactive oxygen species (ROS) level was observed using DCFH-DA, and the mitochondrial superoxide level was observed using MitoSOX Red. Bay K8644 was used to increase the level of intracellular calcium. siRNA was used to interfere with the expression of glycogen synthase kinase (GSK)-3β. Western blot analysis was used to detect the expression of mitochondrial dysfunction-related proteins. The results revealed that oxidative stress decreased mitochondrial membrane potential and increased intracellular ROS, mitochondrial superoxide and cytoplasmic calcium levels in pre-osteoblasts; however, metformin improved mitochondrial dysfunction and reversed oxidative stress-induced injury. Metformin inhibited mitochondrial permeability transition pore opening, suppressed the cytoplasmic calcium influx and reversed pre-osteoblast apoptosis by promoting GSK-3β phosphorylation. Moreover, it was found that EGFR was the cell membrane receptor of metformin in pre-osteoblasts, and the EGFR/GSK-3β/calcium axis played a key role in metformin reversing the oxidative stress response of pre-osteoblasts in post-menopausal osteoporosis. On the whole, these findings provide a pharmacological basis for the use of metformin for the treatment of post-menopausal osteoporosis.

Correspondence to: Professor Yue Zhu or Professor Lin Tao, Department of Orthopedics, First Hospital of China Medical University, 155 Nanjing North Street, Heping, Shenyang, Liaoning 110001, P.R. China
E-mail: zhuyuedr@163.com
E-mail: taolindr@163.com

Abbreviations: ROS, reactive oxygen species; GSK-3β, glycogen synthase kinase 3β; mPTP, mitochondrial permeability transition pore

Key words: osteoporosis, metformin, mitochondrial dysfunction, GSK-3β, EGFR

Introduction

Osteoporosis is a systemic bone disease characterized by a low bone mass and the deterioration of bone tissue microstructure (1). With the aging population, osteoporosis has become one of the major public health concerns worldwide, and osteoporotic fractures have become a main cause of mortality and disability among the elderly (2,3). The maintenance of bone homeostasis requires the balance between bone resorption and bone formation. After the loss of estrogen, this balance is broken, resulting in bone loss, which is the pathogenic mechanism of osteoporosis (4,5). This imbalance may be due to the anti-apoptosis of osteoclasts and the pro-apoptosis of osteoblasts caused by oxidative stress, which is induced by estrogen deficiency, accelerating the rate of bone remodeling (6). Recent research has demonstrated that oxidative stress plays a critical role in the progression of osteoporosis (7). It has been shown that estrogen is an antioxidant, and the increase in oxidation-related biomarkers in post-menopausal women has proven that post-menopausal women with osteoporosis are in a state of oxidative stress (8). Reactive oxygen species (ROS) were previously considered to be exclusively toxic, causing oxidative stress and tissue damage (9). However, it has been proven that a low level of ROS has a signal transduction effect (10). Excessive and abnormal levels of ROS cause molecular damage and initiate the apoptotic process, which is produced mainly due to mitochondrial dysfunction (11). Therefore, the study of osteoporotic drugs targeting mitochondrial dysfunction induced by oxidative stress has promising application prospects.

Over the past 30 years, a range of drugs for the treatment of post-menopausal osteoporosis have been developed and shown to be effective (12). At present, the first-line treatment drugs include bisphosphonates, denosumab, raloxifene and teriparatide (13). However, the rare, yet severe side-effects of bisphosphonates and denosumab are atypical femoral fractures and osteonecrosis of the jaw, which limit their application (14). The long-term use of raloxifene increases the incidence of thromboembolism, and teriparatide can be used for up to 2 years due to its cerebrovascular and central nervous side-effects (3,15). New drug therapies are still being explored (16). Metformin has been used for the treatment of type 2 diabetes for >60 years and is characterized by its safety and low cost (17). At present, the application of metformin in other fields is also being explored, such as for cardiovascular disease, tumors and even aging, with its application involving different mechanisms roles through various signaling pathways (18). It has been demonstrated that metformin exerts a therapeutic effect on osteoporosis induced by diabetes; however, this has focused on the effects of metformin on bone metabolism in a high glucose state (19). However, to date, at least to the best of our knowledge, there are few studies available on whether metformin can reverse post-menopausal osteoporosis induced by oxidative stress (20). At the same time, it is unclear whether metformin can improve pre-osteoblast oxidative stress by reversing mitochondrial dysfunction.

In the present study, a pre-osteoblast model of oxidative stress was constructed to explore the therapeutic effects and mechanisms of action of metformin in post-menopausal osteoporosis. A previous study demonstrated that glycogen synthase kinase (GSK)-3β improved cardiac toxicity caused by ROS and calcium ions (Ca^{2+}) by regulating the mitochondrial permeability transition pore (mPTP) (21). Under conditions of oxidative stress, GSK-3β activates and opens the mPTP, thus inducing calcium overload. It was hypothesized that metformin inactivates GSK-3β via EGFR, which decreases the intracellular Ca^{2+} concentration to attenuate pre-osteoblast apoptosis induced by oxidative stress. To the best of our knowledge, through bioinformatics analyses and experimental verification, the present study, for the first time, examined the entire treatment axis of metformin in post-menopausal osteoporosis. The findings presented herein demonstrate that metformin has potential for use as a safe and effective drug for the treatment of osteoporosis.

Materials and methods

Reagents, cells and cell culture. The MC3T3-E1 cells (GNM15), mouse pre-osteoblast precursors, were obtained The Cell Bank of Type Culture Collection of The Chinese Academy of Sciences. Metformin was obtained from Dalian Meilun Biotechnology Co., Ltd. Primary antibodies against caspase-3 (cat. no. ab184787), Bcl-2 (cat. no. ab182858), BAX (cat. no. ab32503), EGFR (cat. no. ab52894), phosphorylated (p-)EGFR (cat. no. ab52894) and horseradish peroxidase-conjugated anti-rabbit secondary antibodies (cat. no. ab288151) were obtained from Abcam. Primary antibodies against GSK-3β (cat. no. 12456), p-GSK-3β (cat. no. 5558), cleaved caspase-3 (cat. no. 9661), and β-actin (cat. no. 4970) were obtained from Cell Signaling Technology, Inc.

The MC3T3-E1 cells were maintained in α-MEM (HyClone; USA) supplemented with 10% fetal bovine serum (HyClone; Cytiva), 100 U/ml penicillin and 100 mg/ml streptomycin (Corning, Inc.). The cells were cultured in a humidified incubator with 5% CO_2 at 37˚C.

Oxidative damage was induced with 0.2 mM hydrogen peroxide (H_2O_2; 7722-84-1, MilliporeSigma) added to the medium. Following 6 h of treatment, metformin at a concentration of 0.2 mM was added to achieve the optimal effects on the reversal of apoptosis.

Cell viability assay. A Cell Counting Kit-8 (CCK-8) colorimetric assay (APExBIO Technology LLC) was applied to measure cell proliferation and viability. MC3T3-E1 Subclone 14 growth medium (Procell Life Science & Technology Co., Ltd.) containing 89% MEM, 10% FBS, 1% P/S solution. The MC3T3-E1 cells were plated in 100 μl of growth medium/well in 96-well plates (Corning, Inc.) at $5x10^3$ cells/well. The cells were exposed to 0.2 mM H_2O_2 for 6 h and then treated with metformin at 0.2 mM for 48 h at 37˚C. CCK-8 reagent (10 μl/well) was then added to the supernatant followed by incubation for 1 h at 37˚C. The optical density (OD) representing cell viability was measured at 450 nm using an absorbance microplate reader (BioTek Instruments, Inc.).

Apoptosis assay. The apoptosis assay of the MC3T3-E1 cells was performed using a FITC Annexin V Apoptosis Detection kit I (BD Biosciences). A total of $2x10^5$ cells were harvested following treatment with metformin, washed with pre-cooled PBS and centrifuged at 200 x g for 5 min at 4˚C. The cells were resuspended in binding buffer and incubated at room temperature with 5 μl of Annexin V-FITC for 15 min and then with 5 μl of PI for 15 min. Finally, the sample was detected using a flow cytometer, CytoFLEX, (Beckman Coulter, Inc.) and analyzed using CytExpert 2.3 software (Beckman Coulter, Inc.).

Fluorescence inverted microscopy and flow cytometry. JC-1, Fluo-4, DCFH-DA and MitoSOX Red staining (as described below) was examined using a fluorescence inverted microscope (Nikon Eclipse Ti, Nikon Corporation) and a FACScan flow cytometer (Beckman Coulter, Inc.), respectively. A fluorescence inverted microscope was used to observe the intracellular localization and relative qualitative analysis of the markers. Subsequently, flow cytometry was used to detect the average fluorescence intensity of the fluorescence channel where the marker was located via absolute quantitative analysis.

Measurement of mitochondrial membrane potential. The mitochondrial membrane potential of the MC3T3-E1 cells was examined using a mitochondrial membrane potential assay kit with JC-1 (Beyotime Institute of Biotechnology). A total of $2x10^5$ cells were mixed well with 1 ml of JC-1 dye working solution and then incubated at 37˚C for 20 min. After washing twice with JC-1 dyeing buffer, the sample was detected using a FACScan flow cytometer. The red fluorescence at 590 nm was accepted via the PE channel, while the green fluorescence at 520 nm was accepted via the FITC channel. The red/green fluorescence ratio was used to represent the mitochondrial membrane potential level. The decrease in the red/green ratio indicated the openness of the mPTP.

Detection of the intracellular calcium concentration. The concentration of intracellular Ca^{2+} in the MC3T3-E1 cells was examined using Fluo-4 AM (Beyotime Institute of Biotechnology). The cells inoculated in 24-well plates were washed three times with PBS to ensure that the medium was completely removed. Subsequently, the cells were completely covered with 300 μl Fluo-4 AM working solution and incubated at 37˚C for 30 min. After washing twice with PBS, the cells were incubated for a further 30 min to ensure that the Fluo-4 AM in the cells was completely transformed into Fluo-4 with fluorescence. The fluorescence intensity of intracellular Fluo-4 was measured, which represented the concentration of Ca^{2+}. Bay K8644 (Dalian Meilun Biology Technology Co., Ltd.), as a highly selective L-type calcium channel agonist, was used to increase cytoplasmic calcium concentration. Bay K8644 at a concentration of 10 μM was added to the MC3T3-E1 cells with metformin and incubated for 48 h at 37˚C.

Detection of ROS. The MC3T3-E1 cells were inoculated in 24-well plates and examined using a ROS assay kit (Beyotime Institute of Biotechnology) following exposure to H_2O_2 and treatment with metformin. DCFH-DA was diluted with serum-free culture medium at a 1:1,000 ratio to prepare the working solution. The cells to be tested were covered with diluted DCFH-DA and incubated in a cell incubator at 37˚C for 30 min. The fluorescence intensity of DCFH-DA was measured to represent the content of intracellular ROS.

Detection of mitochondrial superoxide. Superoxide in the mitochondria was detected using the MitoSOX Red mitochondrial superoxide indicator (Shanghai Yeasen Biotechnology Co., Ltd.). The dry powder of the probe was diluted with DMSO as the storage solution, which was diluted 1,000-fold with PBS to yield a 5-μm MitoSOX Red working solution. The MC3T3-E1 cells were inoculated in a 24-well plate and washed with PBS at 37˚C. Subsequently, 300 μl of working solution were added to each well and incubated at 37˚C away from light for 10 min. The fluorescence intensity of MitoSOX Red was measured to represent the content of superoxide in the mitochondria.

Cellular immunochemical analysis. The MC3T3-E1 cells were first treated with 0.1% Triton X-100 (Beyotime Institute of Biotechnology) to increase the cell membrane permeability and then fixed with 4% paraformaldehyde at room temperature for 30 min. The fixed cell climbing tablets were covered by sufficient primary antibody of GSK-3β diluted at 1/200 and incubated at 4˚C away from light overnight. Following thorough cleaning with PBST, the cells were incubated in fluorescently labeled secondary antibody (Alexa Fluor® 594, cat. no. ab150080, Abcam) diluted at 1/200 for 1 h in the dark. Finally, the cells were treated with DAPI (Beyotime Institute of Biotechnology) to stain the nuclei for 5 min at room temperature and observed under a fluorescence microscope (Nikon Eclipse Ti, Nikon Corporation).

Enrichment analysis of Gene Ontology (GO) and Kyoto Encyclopedia of Genes and Genes (KEGG) pathways. The present study analyzed the transcriptome data (GSE198254) of metformin reversing osteoporosis in pre-osteoblasts (22). Gene Set Enrichment Analysis (GSEA) of differentially expressed genes (DEGs) was carried out using clusterProfiler R statistical software (R, x64, 4.1.3). The GO database was used to annotate genes from three aspects: Biological process (BP), molecular function (MF) and cellular component (CC). At the same time, the KEGG database was used to analyze the top enrichment pathway involved in the effects of metformin against osteoporosis induced by oxidative stress. The ggplot2 package (http://ggplot2.tidyverse.org) was used to visualize the results.

Western blot analysis. The cells to be tested were treated with radioimmunoprecipitation assay (RIPA) buffer (Beyotime Institute of Biotechnology) on ice for 30 min and then lysed under ultrasound to obtain complete lysate. The pyrolysis product was centrifuged at 4˚C for 10 min at 10,000 x g, and the supernatant was then collected. A BCA assay kit (Beyotime Institute of Biotechnology) was used to detect the protein concentration. Electrophoresis was performed using 10% SDS-PAGE and the proteins were then transferred onto polyvinylidene difluoride membranes (PVDF). After blocking with 5% BSA on a shaking table at room temperature for 1 h, the membranes were incubated with the primary antibodies overnight. After cleaning with TBST, the membranes were incubated with the secondary antibody for 1 h at 4˚C. Primary antibodies against GSK-3β, p-GSK-3β, cleaved caspase-3, caspase-3, Bcl-2, BAX, EGFR, p-EGFR, β-actin were diluted at 1/3,000. Horseradish peroxidase-conjugated anti-rabbit secondary antibodies was diluted at 1/2,000. β-actin (43 kDa) was used as the standard for protein levels. The protein bands that were fully immersed in the enhanced chemiluminescence (ECL) were visualized using the chemiluminescence imaging system (Analytik Jena Ag). Finally, the quantified optical density was calculated using ImageJ v1.8.0 software (National Institutes of Health).

siRNA transfection. GSK-3β-small interfering RNAs (siRNAs) were purchased from Synbio-tech Suzhou Co., Ltd. Three siRNAs were transfected at the same time, and the content of GSK-3β was detected using western blot analysis to reflect the transfection efficiency. MC3T3-E1 cells transfected with negative siRNAs was as a negative control. GSK-3β-si-1 was selected for use in subsequent experiments as the content of GSK-3β was the lowest. The MC3T3-E1 cells were inoculated into six-well plates at a cell density of 50% when transfected 24 h later. siRNA at 50 nM and Lipofectamine™ 3000 reagent (Thermo Fisher Scientific, Inc.) were prepared in antibiotic-free Opti-MEM (Thermo Fisher Scientific, Inc.) and then mixed at room temperature for 20 min. Finally, the cells were treated with siRNA transfection reagent for 6 h, then change fresh medium for incubation for 48 h in the 37˚C incubator. The siRNA sequences are listed in Table I.

Statistical analysis. An unpaired Student's t-test was used to examine relative protein expression in cells transfected with siRNA against GSK-3β and one-way ANOVA followed by Tukey's post hoc test was used to determine significant differences between multiple treatment groups. $P<0.05$ was considered to indicate a statistically significant difference. All experiments were repeated three times and analyzed using SPSS 19.0 software (IBM Corp).

Table I. RNA interference sequences used for transfection.

Name	Forward (5'-3')	Reverse (5'-3')
GSK-3β-si-1	GAAAGUUAGCAGAGAUAAATT	UUUAUCUCUGCUAACUUUUCTT
GSK-3β-si-2	AGAAAGUUCUACAGGACAATT	UUGUCCUGUAGAACUUUCUTT
GSK-3β-si-3	CAAAUUAUACAGAAUUCAATT	UUGAAUUCUGUAUAAUUUGTT

GSK-3β, glycogen synthase kinase 3β.

Results

Metformin reverses pre-osteoblast mitochondrial dysfunction by attenuating mPTP opening. Based on a previous study by the authors, 0.2 mM was determined to be the optimal concentration of H_2O_2 to induce oxidative stress in pre-osteoblasts, which reached the maximum apoptotic rate (22). In addition, 0.2 mM metformin was shown to have the strongest ability to reverse oxidative apoptosis (22). The present study first examined the mechanisms by which metformin prevents pre-osteoblast apoptosis. The transcriptome data (GSE198254) of ovariectomized (OVX) mice treated with and without metformin were analyzed and GSEA was performed using the R software package (clusterProfiler) (23). Functional enrichment (GO) analysis revealed that in the CC category, DEGs were mainly enriched in mitochondrial components (mitochondrial inner membrane and mitochondrial protein-containing complex). In the MF category, DEGs were closely related to transcriptional regulation (transcription coregulator activity and catalytic activity, acting on RNA). In the BP category, DEGs were mainly enriched in protein modification (negative regulation of protein modification process and regulation of protein stability) (Fig. 1A). To further examine the effects and pathways through which metformin affects mitochondrial function, the openness of the mPTP was examined. With a decrease in mitochondrial membrane potential, the JC-1 monomer enters the cytoplasm through the open mPTP, while it exists in the form of a polymer within healthy mitochondria (24). JC-1 was observed in the cytoplasm using fluorescence microscopy and it was found that the ratio of red/green fluorescence was decreased in MC3T3-E1 cells exposed to H_2O_2. Similarly, this effect was attenuated by metformin, suggesting that metformin prevented mitochondrial dysfunction by controlling mPTP opening (Fig. 1B and C). During this process, the level of intracellular ROS was consistent with the opening of the mPTP (Fig. 1D and E).

Metformin reverses pre-osteoblast mitochondrial apoptosis by reducing the cytoplasmic calcium concentration through the mPTP. The present study further examined whether metformin regulates apoptosis through calcium. It was found that in the H_2O_2 group, the concentration of Ca^+ increased significantly, and metformin reversed this effect. Following the addition of the calcium channel agonist, Bay K8644, the calcium concentration increased compared with that in the H_2O_2 + metformin group (Fig. 2A and B). Furthermore, the apoptotic rate of MC3T3-E1 cells was measured during this process. In the H_2O_2 group, the apoptotic rate increased, metformin reversed pre-osteoblast apoptosis, and Bay K8644 attenuated the protective effects of metformin (Fig. 2C and D). The results of western blot analysis also revealed that the levels of mitochondrial apoptosis-related proteins were altered: The levels of BAX and cleaved caspase-3 were increased, while those of BCL-2 were decreased in the cell model of oxidative stress induced by H_2O_2. These changes were reversed by metformin and Bay K8644 attenuated the effects of metformin (Fig. 2E and F).

Metformin attenuates pre-osteoblast apoptosis induced by oxidative stress through GSK-3β. To examine the mechanisms through which metformin ameliorates mitochondrial dysfunction and attenuates apoptosis, GSK-3β was selected from the genes involved in the negative regulation of protein modification, as determined using GO enrichment analysis; GSK-3β is involved in regulating the mPTP in mitochondria (25). GSEA revealed that metformin promoted the negative regulation of protein modification (Fig. S1). The expression of GSK-3β was observed using fluorescence inverted microscopy. Contrary what was initially expected, metformin and oxidative stress did not markedly increase the levels of GSK-3β. However, it was found that the fluorescence in the control group was evenly distributed, while there was localized fluorescence in the H_2O_2 and metformin groups (Fig. 3A). It was hypothesized that GSK-3β may accumulate in organelles under conditions of oxidative stress. To further clarify the role of GSK-3β in the metformin-mediated reversal of pre-osteoblast apoptosis induced by oxidative stress, GSK-3β was knocked down using siRNA (Fig. 3B). It was found that the knockdown of GSK-3β prevented metformin from reversing apoptosis (Fig. 3C). The levels of ROS in the cytoplasm were also measured (Fig. 3D and E), which confirmed the reversal of oxidative stress by metformin and the loss of the antioxidant effects following the knockdown of GSK-3β. Finally, the expression of mitochondrial apoptosis marker proteins was detected using western blot analysis (Fig. 3F). The results revealed that the BAX and cleaved caspase-3 expression levels were higher in the metformin treatment group following GSK-3β knockdown than in the group treated with metformin and not subjected to GSK-3β knockdown, while BCL-2 expression was lower. These results thus revealed that GSK-3β was involved in the anti-apoptotic effects of metformin by improving mitochondrial dysfunction, although this effect was not related to the expression of GSK-3β. It was hypothesized that metformin may protect pre-osteoblast mitochondria and may prevent apoptosis by regulating the activity of GSK-3β.

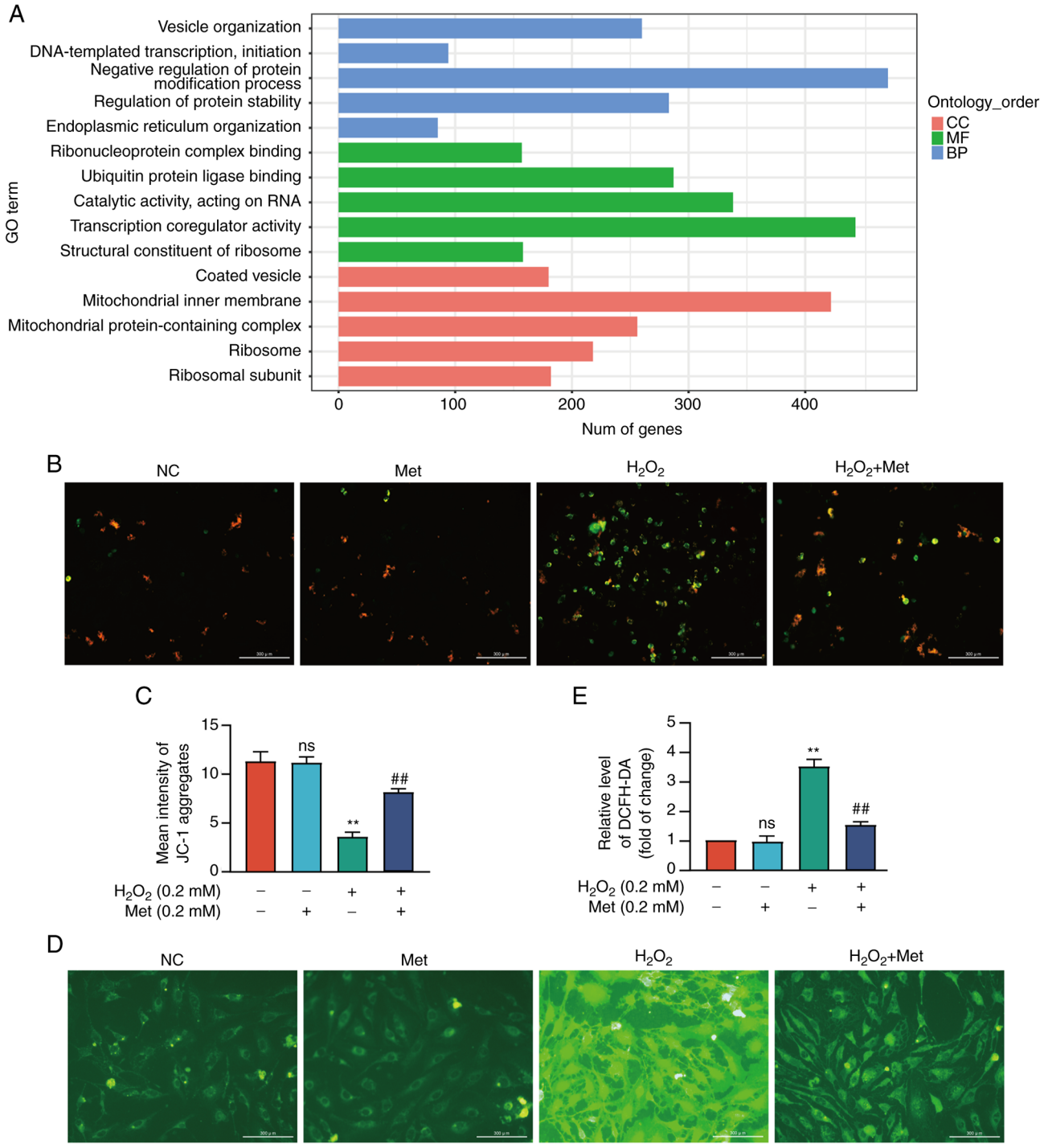

Figure 1. Metformin reverses pre-osteoblast mitochondrial apoptosis by attenuating mitochondrial permeability transition pore opening. (A) Metformin in the process of cytological components, molecular biological functions and biological processes through GO analysis. (B) The number of JC-1 monomers and JC-1 aggregates in MC3T3-E1 cells with or without metformin treatment was observed. (C) The fluorescence intensity of JC-1 aggregates was detected using a full-wavelength multifunctional microplate reader. The fluorescence intensity decreased in the H_2O_2 group, and metformin group reversed this process. (D) The intracellular ROS level was observed using a fluorescence electron microscope. (E) The average fluorescence intensity was detected using flow cytometry. ROS generation increased in H_2O_2 group and decreased in the metformin group. The experiment was conducted three times. The data are expressed as the mean ± SD. **P<0.01, compared with the control cells; $^{\#\#}$P<0.01, compared with the H_2O_2 group. ns, not significant; GO, Gene Ontology; CC, cellular component; MF, molecular function; BP, biological process; ROS, reactive oxygen species; Met, metformin; H_2O_2, hydrogen peroxide.

Metformin inhibits mPTP opening and Ca^{2+}-mediated mitochondrial dysfunction through GSK-3β. Subsequently, the present study observed changes in mitochondrial membrane potential to determine the openness of the mPTP (Fig. 4A and B). Furthermore, changes in the Ca^{2+} concentration in the cytoplasm during this process were measured (Fig. 4C, E and G). The results revealed that H_2O_2 induced oxidative stress, mPTP opening and an increase in the Ca^{2+} concentration in MC3T3-E1 cells; these effects were reversed by metformin. Following the knockdown of GSK-3β, metformin could not reverse mPTP opening or the increase in Ca^{2+} concentrations. Furthermore, the level

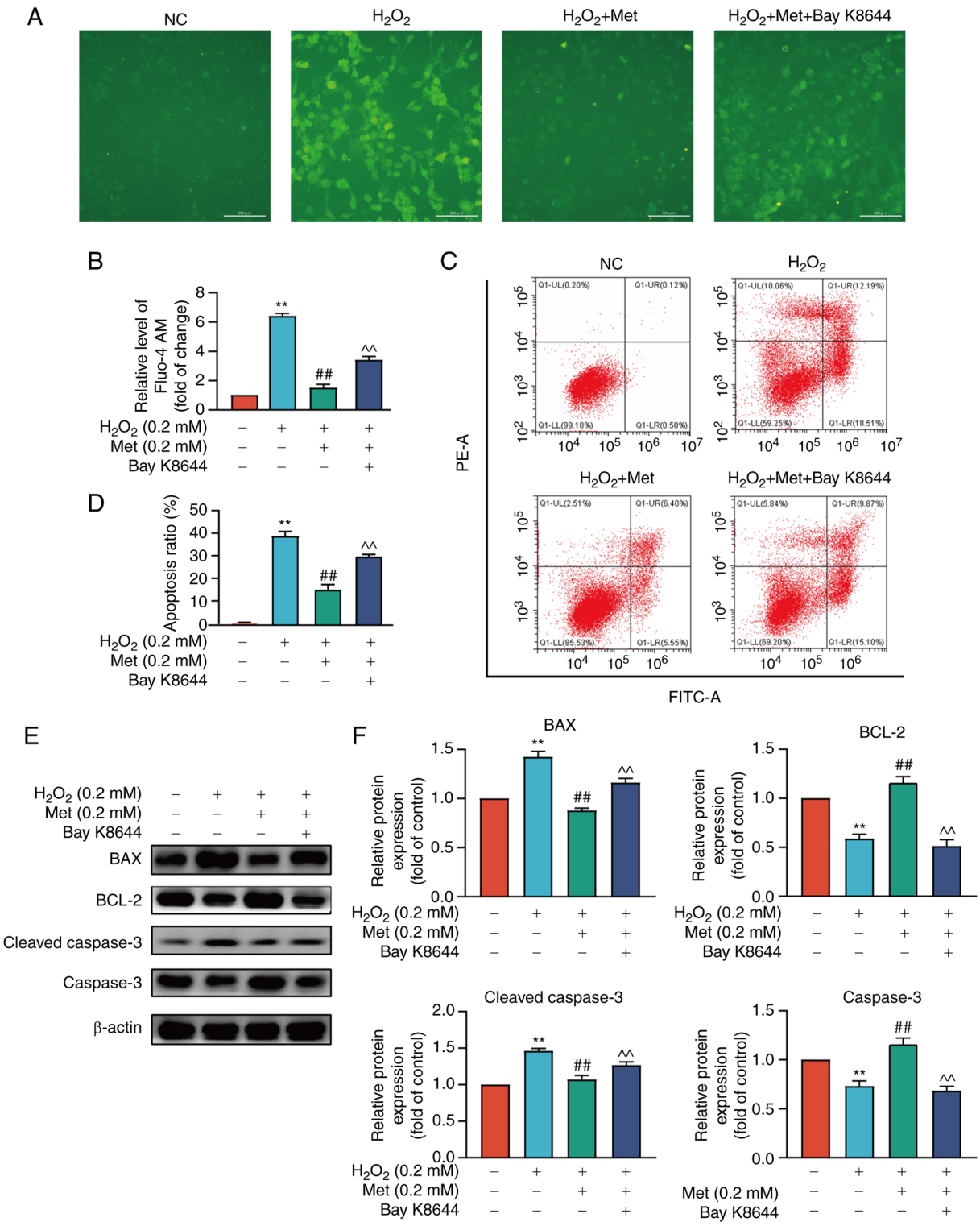

Figure 2. Metformin reverses pre-osteoblast mitochondrial apoptosis by reducing the cytoplasmic calcium concentration through the mitochondrial permeability transition pore. (A) The intracellular calcium was observed using a fluorescence electron microscope. (B) The average fluorescence intensity was detected using flow cytometry. (C) The apoptotic rate was detected using flow cytometry. The apoptotic rate of the H_2O_2 group was 30.70%, that of the H_2O_2 + metformin group was 11.95%, and that of the H_2O_2 + metformin + Bay K8644 group was 24.97%. (D) Apoptotic rate of MC3T3-E1 cells exposed to by H_2O_2 and treated with metformin. (E) The expression of mitochondrial apoptosis-related proteins was detected using western blot analysis. (F) The protein expression of BAX/BCL-2/cleaved caspase-3/caspase-3 compared with the control group was examined. The experiments were performed three times. Data are presented as the mean ± SD. **P<0.01, compared with the control cells; $^{\#\#}$P<0.01, compared with the H_2O_2 group; $^{\wedge\wedge}$P<0.01, compared with the H_2O_2 + Met group. Met, metformin; H_2O_2, hydrogen peroxide.

of superoxide in mitochondria was measured to determine mitochondrial dysfunction (Fig. 4D, F and H). It was found that H_2O_2 increased the mitochondrial superoxide levels and metformin decreased the superoxide levels; the superoxide levels increased following the knockdown of GSK-3β. This finding was consistent with the hypothesis that metformin

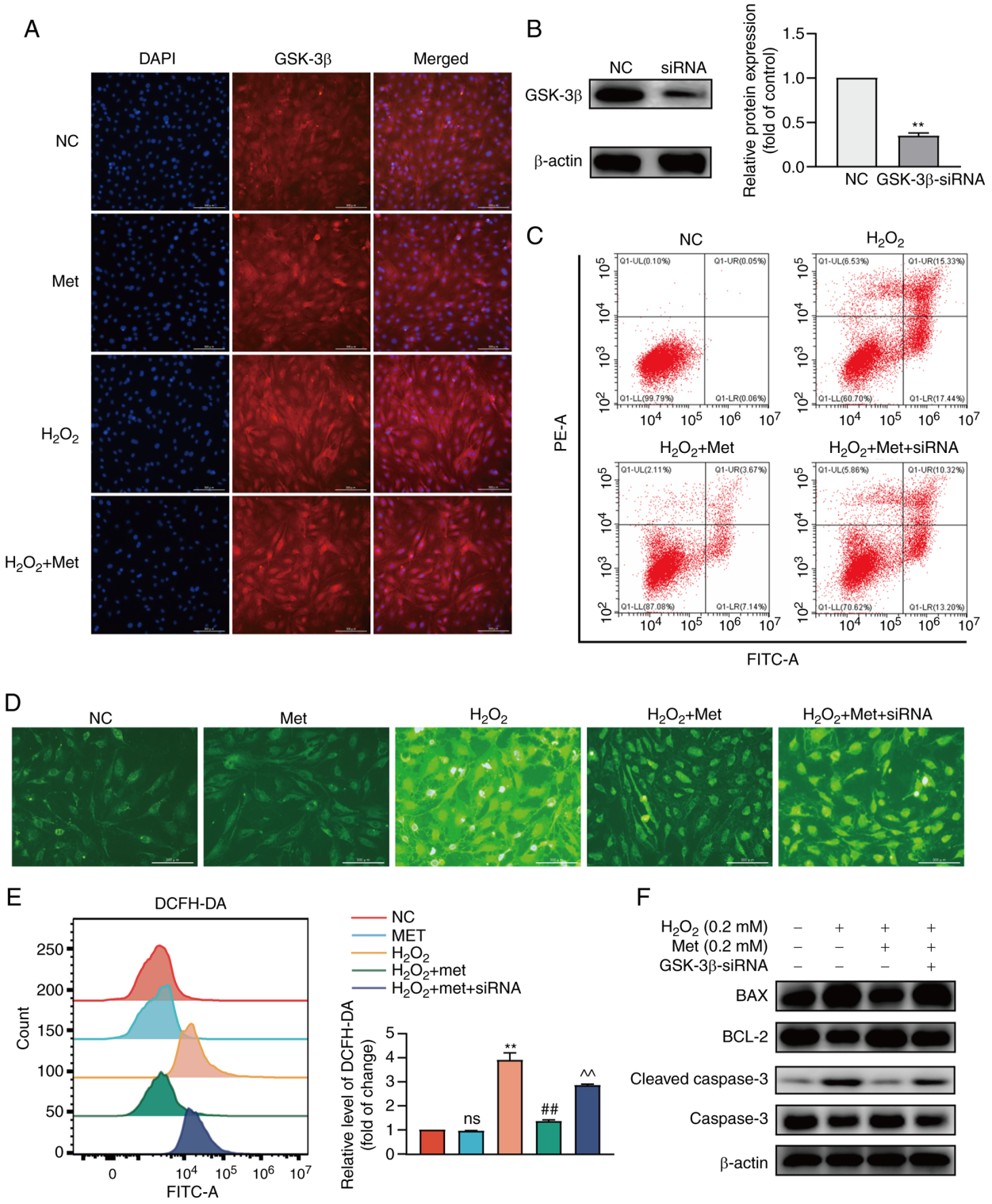

Figure 3. Metformin improves pre-osteoblast apoptosis induced by oxidative stress through GSK-3β. (A) The localization and expression of GSK-3β was observed in MC3T3-E1 cells and GSK-3β was in a more aggregated state. (B) The silencing efficiency of GSK-3β was detected at the protein level. (C) The apoptotic rate after the silencing of GSK-3β was detected. The apoptotic rate of the H_2O_2 group was 32.77%, that of the H_2O_2 + metformin group was 10.81%, and that of the H_2O_2 + metformin + siRNA group was 23.52%. (D) The level of ROS in the cytoplasm was detected before and after treatment with metformin and siRNA-GSK-3β. (E) The fluorescence intensity of ROS was detected using flow cytometry. (F) The expression of mitochondrial apoptosis-related proteins after the silencing of GSK-3β was detected again. The experiments were performed three times. Data are presented as the mean ± SD. **P<0.01, compared with the control cells; $^{\#\#}$P<0.01, compared with the H_2O_2 group; $^{\wedge\wedge}$P<0.01, compared with the H_2O_2 + Met group. ns, not significant; ROS, reactive oxygen species; Met, metformin; H_2O_2, hydrogen peroxide; GSK-3β, glycogen synthase kinase 3β.

inhibited mPTP opening, weakened the cytoplasmic calcium influx, attenuated mitochondrial superoxide damage to the mitochondria and reversed apoptosis via GSK-3β.

Metformin reverses pre-osteoblast apoptosis induced by oxidative stress by phosphorylating GSK-3β via the EGFR pathway. Finally, the present study examined whether the

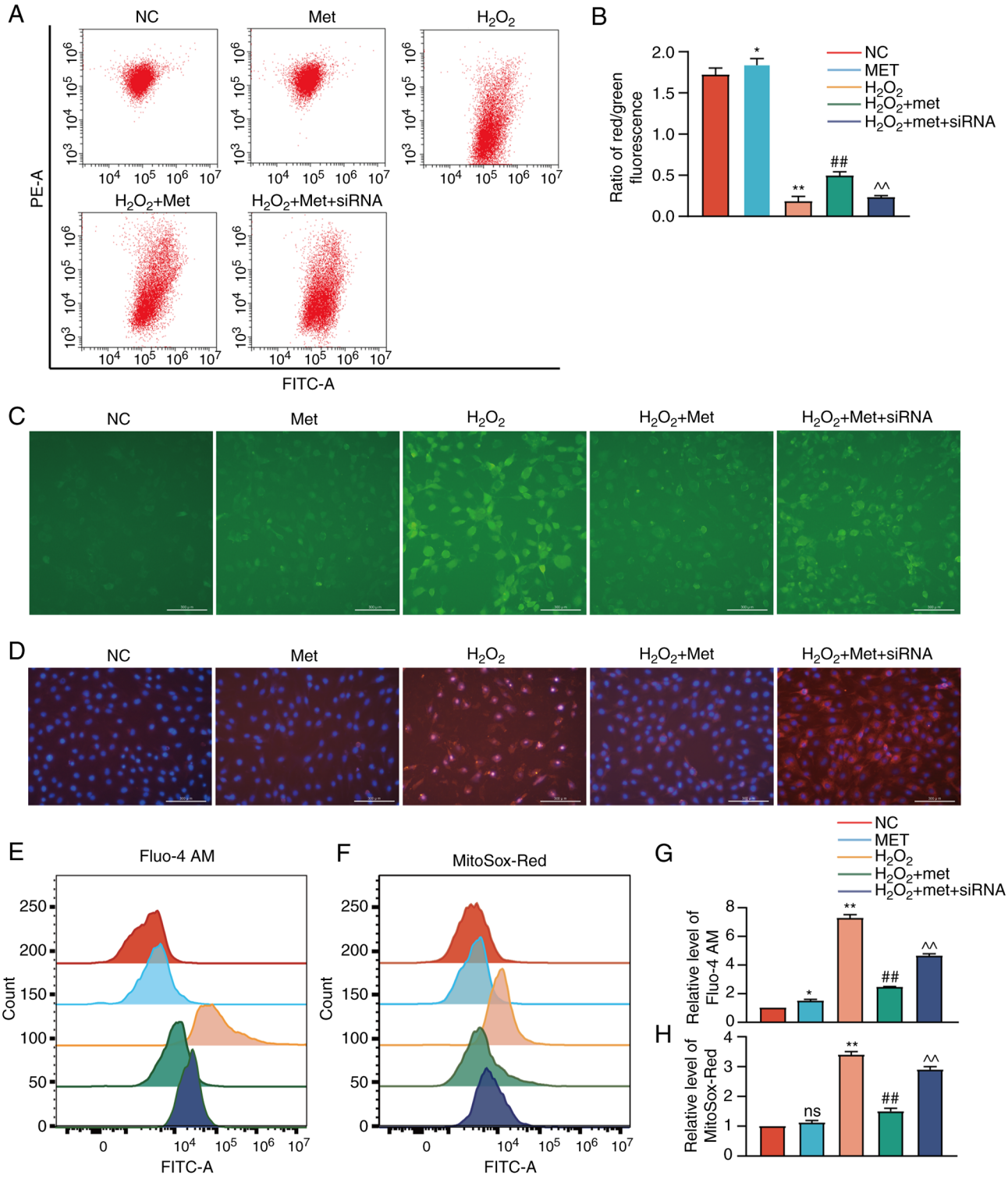

Figure 4. Metformin inhibits mPTP opening and Ca2+-mediated mitochondrial dysfunction via GSK-3β. (A) The effect of Met on mitochondrial membrane potential in MC3T3-E1 cells was detected. (B) The ratio of red/green fluorescence representing mitochondrial membrane potential was quantitatively analyzed using flow cytometry. (C) Intracellular calcium was observed using a fluorescence electron microscope. (D) Mitochondrial superoxide was observed using a fluorescence electron microscope. Blue fluorescence indicates DAPI, and red fluorescence indicates mitochondrial superoxide. (E) Quantitative analysis of calcium fluorescence intensity using flow cytometry. (F) Quantitative analysis of fluorescence intensity of mitochondrial superoxide using flow cytometry. (G) Quantitative analysis of the levels of calcium. (H) Quantitative analysis of the levels of mitochondrial superoxide. The experiments were performed three times. Data are presented as the mean ± SD. *P<0.05 and **P<0.01, compared with the control cells; $^{\#\#}$P<0.01, compared with the H_2O_2 group; $^{\wedge\wedge}$P<0.01, compared with the H_2O_2 + Met group. ns, not significant; Met, metformin; H_2O_2, hydrogen peroxide; GSK-3β, glycogen synthase kinase 3β.

regulation of GSK-3β by metformin was mediated by the level of phosphorylation. The results of western blot analysis revealed that metformin markedly increased GSK-3β phosphorylation, which was consistent with the antioxidant level (Fig. 5A). The results of pathway enrichment analysis (KEGG) revealed that the DEGs were closely related to the ErbB signaling pathway

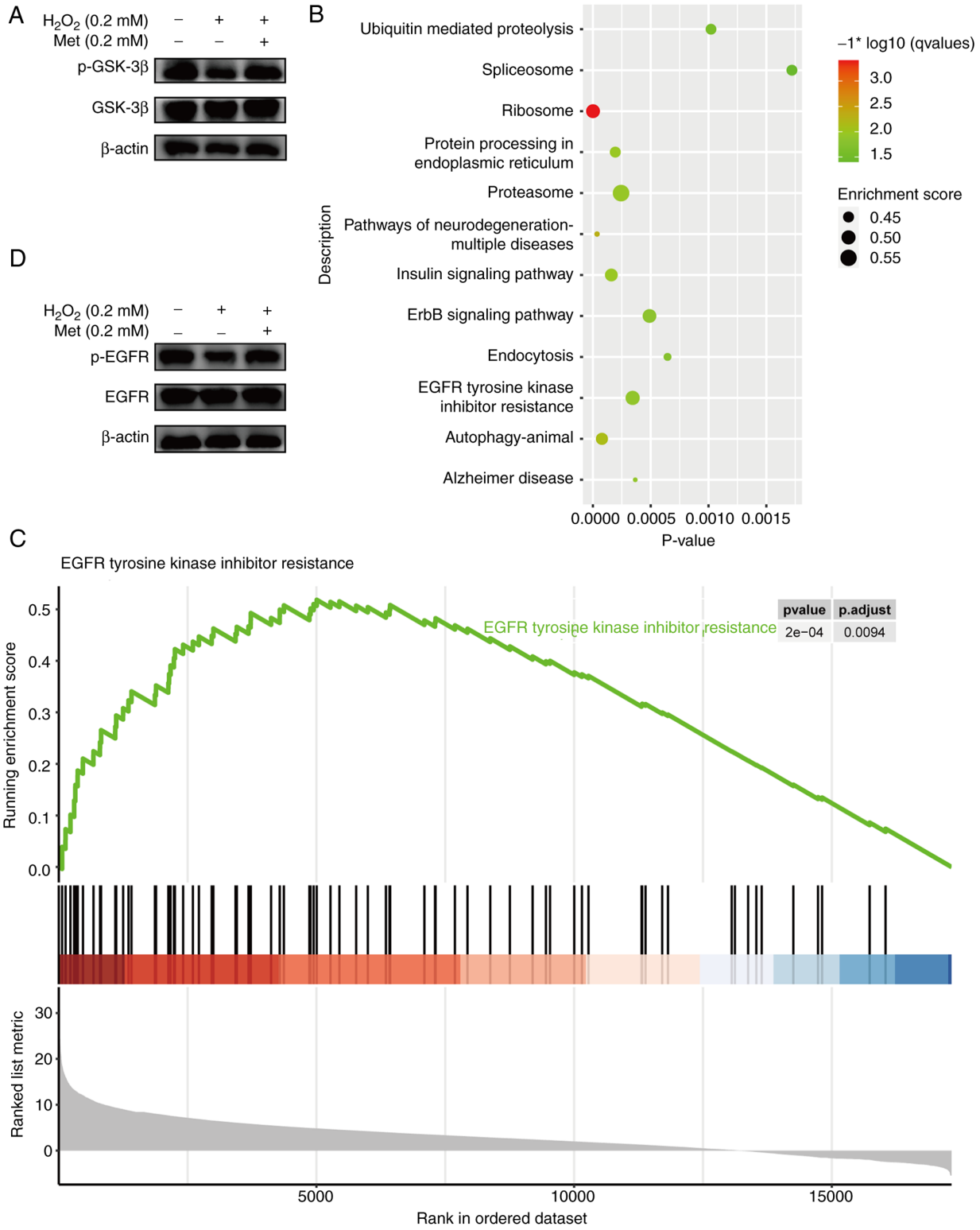

Figure 5. Metformin reverses pre-osteoblast apoptosis induced by oxidative stress by phosphorylating GSK-3β via the EGFR pathway. (A) The effect of metformin on the phosphorylation level of GSK-3β was detected at the protein level. (B) The KEGG pathway of differentially expressed genes in OVX vs. OVX + Met. The EGFR pathway has a lower P-value and better enrichment. OVX represents post-menopausal osteoporosis mice. (C) The expression and regulation of EGFR was examined using gene set enrichment analysis. (D) The phosphorylation level of EGFR was detected at the protein level. GSK-3β, glycogen synthase kinase 3β.

and EGFR tyrosine kinase inhibitor resistance (Fig. 5B). It was found that the metformin group had an upregulated EGFR tyrosine kinase inhibitor resistance pathway (Fig. 5C). ErbB is a member of the EGFR family (26). Moreover, some studies have shown that EGFR is involved in the regulation of GSK-3β activity in tumors (27). Therefore, it was hypothesized that metformin can affect pre-osteoblast apoptosis through the EGFR pathway. The present study measured the expression of

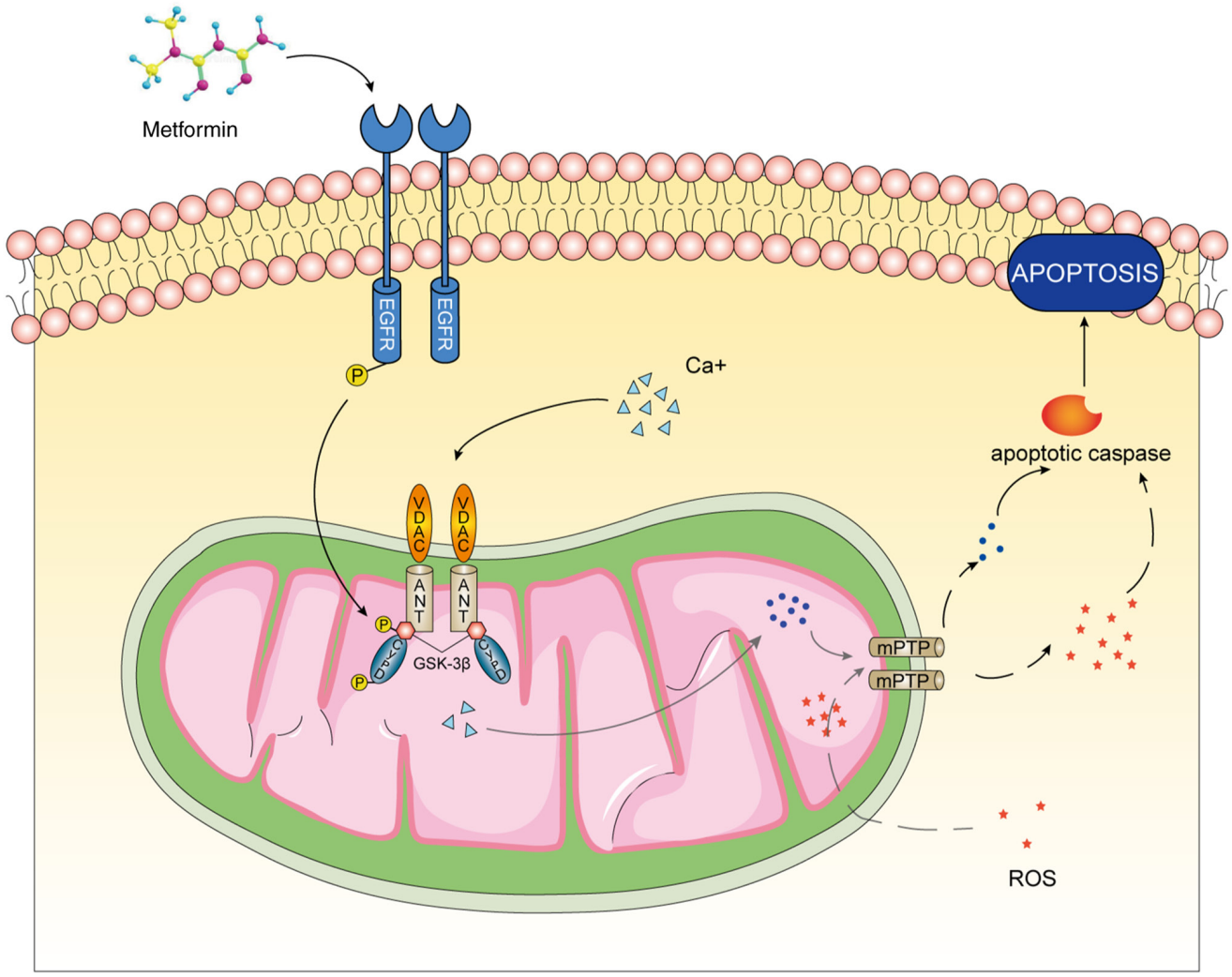

Figure 6. Flow chart of metformin regulating the mPTP of MC3T3-E1 cells through the EGFR/GSK-3β/calcium axis and reversing osteoporosis caused by oxidative stress. ROS, reactive oxygen species; GSK-3β, glycogen synthase kinase 3β; mPTP, mitochondrial permeability transition pore.

EGFR and p-EGFR in each group using western blot analysis. The results revealed that oxidative stress inhibited the phosphorylation of EGFR, while metformin reversed this change (Fig. 5D). These results indicate that metformin affects the activity of GSK-3β through the EGFR pathway and improves mitochondrial dysfunction to prevent MC3T3-E1 apoptosis caused by oxidative stress.

Discussion

Metformin is one of the most widely used oral hypoglycemic drugs in clinic practice, and its safety has been verified (28). At the same time, metformin exhibits prominent anti-inflammatory potential and regulates cell aging, apoptosis and macromolecular damage (29). Following menopause, the body is in a state of high oxidation, which is the main factor leading to bone aging and osteoporosis (30). Through the construction of a pre-osteoblast oxidative stress model, the present study confirmed that metformin improved the oxidation state of MC3T3-E1 cells and reversed the occurrence of apoptosis by reversing mitochondrial dysfunction, clarifying the underlying mechanisms. Metformin has been shown to be beneficial in attenuating the hallmarks of aging (31). Mitochondria are the key organelles regulating cellular life and participate in the functional regulation of energy metabolism, calcium signal transduction, cell homeostasis and apoptosis (32). An increasing number of studies have proven that apoptosis is attributed to the internal killing mechanism of mitochondria and is the key factor in osteoporosis (33). The present study further proposed that the mPTP plays a major role. mPTP is a group of non-specific pores formed by protein complexes between the inner and outer membranes of the mitochondria, which maintains the proton barrier and energy metabolism balance of the mitochondria (34). At the same time, calcium, as a second messenger, plays a precise regulatory role in pre-osteoblast apoptosis induced by oxidative stress (35). During oxidative stress, calcium accumulates in the cytoplasmic matrix from the endoplasmic reticulum or extracellular matrix, causing calcium overload (36,37). The present study found that calcium overload occurred during oxidative stress, while metformin decreased the calcium levels. The addition of Bay K8644 increased the level of intracellular calcium and attenuated the ability of metformin to reverse pre-osteoblast apoptosis. It was suggested that metformin regulates apoptosis

by regulating mPTP opening and controlling the Ca^{2+} influx in MC3T3-E1 cells.

The present study then investigated the mechanism through which metformin regulates mPTP opening. GSK-3β is a Ser/Thr kinase widely present in the cytoplasmic matrix, nucleus and mitochondria. Originally, it was identified as a rate-limiting enzyme for glycogen synthesis. Subsequently, it was found to affect a variety of cellular processes, including embryonic development, cell growth, differentiation, apoptosis and the stress response (38,39). The mPTP is composed of the ion channel VDAC of the mitochondrial outer membrane, the mitochondrial inner membrane transporter (ANT) and cyclophilin D (CypD) (40). Among these, CypD is a functional regulator of mPTP, which triggers the conformational change of mPTP by combining with ANT (41). Recent research has found that CypD is also a phosphorylation substrate of GSK-3β. The phosphorylation of CypD increases binding with ANT, which increases the sensitivity of mPTP to Ca^{2+} and reduces the threshold of mPTP opening (42). The present study found that in pre-osteoblasts exposed to H_2O_2, the total amount of GSK-3β remained unaltered, although the level of p-GSK-3β decreased, accompanied by the opening of the mPTP and increases in Ca^{2+}, intracellular ROS and mitochondrial superoxide. It has been shown that GSK-3β is active in the physiological state and inactivated following phosphorylation (43). This is consistent with the results obtained herein, in that following treatment with metformin, GSK-3β phosphorylation increased, and inactivated GSK-3β decreased the binding ability of CypD to ANT, thereby inhibiting mPTP opening.

Although GSK-3β plays a role in the intracellular mitochondria, the mechanisms through which metformin communicates extracellular signals to GSK-3β warrants further clarification (44). The present study further explored the enzyme-mediated pathway by which metformin regulates GSK-3β from the extracellular space to the mitochondria. GSEA of GO and KEGG was carried out on the transcriptome data of OVX and (OVX + Met) osteoporosis model mice. It was found that metformin was related to the composition of the mitochondria (mitochondrial inner membrane, mitochondrial protein-containing complex) in the cytological components. GSK-3β was involved in upregulating the negative expression of protein modification in biological processes, which also suggest that metformin might have inhibited the opening of mPTP by modifying CypD. It was found that DEGs were highly enriched in the EGFR signaling pathway and upregulated the phosphorylation of EGFR by tyrosine kinase in KEGG. EGFR signaling is closely related to life processes, such as angiogenesis, tumor invasion, metastasis and apoptosis (45). At the same time, it has been found that EGFR-specific inhibitors reduce the number of bone marrow mesenchymal progenitor cells and lead to cortical bone degeneration (46). The present study further confirmed that metformin significantly increased EGFR phosphorylation in pre-osteoblasts exposed to oxidative stressed and that EGFR was the membrane receptor of metformin on pre-osteoblasts. It is suggested that metformin can regulate the mPTP of MC3T3-E1 through the EGFR/GSK-3β/calcium axis and reverse osteoporosis induced by oxidative stress (Fig. 6).

The present study first proposed the therapeutic effects of GSK-3β on osteoporosis induced by oxidative stress by regulating mPTP. At the same time, the EGFR/GSK-3β/calcium axis plays a crucial role in this process. As the direct use of mPTP inhibitors will produce various side-effects in patients (47), GSK-3β will be another target for the treatment of osteoporosis in the future. However, a limitation of the present study is that GSK-3β has a wide range of substrates and targeting only the mitochondria can reduce side-effects and improve the effects. It was found that GSK-3β in the cytoplasm underwent mitochondrial translocation in response to oxidative stress and metformin treatment. This may be related to the N-terminal domain of GSK-3β, which may be used as a target sequence of the mitochondria (48). In the future, further research on the structure of GSK-3β is required to realize the targeted inhibition of the mitochondria, which will be the key to the treatment of diseases caused by oxidative stress.

In conclusion, the present study demonstrated that metformin reversed oxidative stress-induced mitochondrial dysfunction in pre-osteoblasts via the EGFR/GSK-3β/calcium pathway. Moreover, GSK-3β has potential for use as a key target for the treatment of osteoporosis in the future. A limitation of the present study however, was that although the concentration of 0.2 mM H_2O_2 was too high for clinical use, MC3T3-E1 cells reached the maximum apoptotic rate at the concentration. Herein, 0.2 mM was used to establish the osteoporosis model at the cellular level.

Acknowledgements

Not applicable.

Funding

The present study was supported by the National Natural Science Foundation of China (grant no. 81472044) and the Science and Technology Planning Project in Shenyang (grant no. 20-205-2-045).

Availability of data and materials

The datasets used and/or analyzed during the current study are available from the corresponding author on reasonable request.

Authors' contributions

FC was involved in data curation and in the study methodology, as well as in the writing of the original draft. KY was involved in data curation and in the study methodology, as well as in the provision of software. SQ was involved in the conceptualization of the study, and in the writing of the original draft. JL was involved in the investigative aspects of the study and in data curation. WJ was involved in the investigative aspects of the study and in the provision of software. LT was involved in the conceptualization of the study, as well as in data validation, and in the writing, reviewing and editing of the manuscript. YZ was involved in funding acquisition, in the provision of resources, project administration, in the writing of the manuscript, and in the conception and design of the study. All authors have approved the final manuscript and confirm the authenticity of all the raw data.

Ethics approval and consent to participate

Not applicable.

Patient consent for publication

Not applicable.

Competing interests

The authors declare that they have no competing interests.

References

1. Bandeira L and Bilezikian JP: Novel therapies for postmenopausal osteoporosis. Endocrinol Metab Clin North Am 46: 207-219, 2017.
2. Kanis JA, Cooper C, Rizzoli R and Reginster JY; Scientific Advisory Board of the European Society for Clinical and Economic Aspects of Osteoporosis (ESCEO) and the Committees of Scientific Advisors and National Societies of the International Osteoporosis Foundation (IOF): European guidance for the diagnosis and management of osteoporosis in postmenopausal women. Osteoporos Int 30: 3-44, 2019.
3. Black DM and Rosen CJ: Clinical practice. Postmenopausal osteoporosis. N Engl J Med 374: 254-262, 2016.
4. Kespohl B, Schumertl T, Bertrand J, Lokau J and Garbers C: The cytokine interleukin-11 crucially links bone formation, remodeling and resorption. Cytokine Growth Factor Rev 60: 18-27, 2021.
5. Appelman-Dijkstra NM and Papapoulos SE: Modulating bone resorption and bone formation in opposite directions in the treatment of postmenopausal osteoporosis. Drugs 75: 1049-1058, 2015.
6. Li J, Li X, Liu D, Hamamura K, Wan Q, Na S, Yokota H and Zhang P: eIF2α signaling regulates autophagy of osteoblasts and the development of osteoclasts in OVX mice. Cell Death Dis 10: 921, 2019.
7. Zhao F, Guo L, Wang X and Zhang Y: Correlation of oxidative stress-related biomarkers with postmenopausal osteoporosis: A systematic review and meta-analysis. Arch Osteoporos 16: 4, 2021.
8. Mohamad NV, Ima-Nirwana S and Chin KY: Are oxidative stress and inflammation mediators of bone loss due to estrogen deficiency? A review of current evidence. Endocr Metab Immune Disord Drug Targets 20: 1478-1487, 2020.
9. Vatner SF, Zhang J, Oydanich M, Berkman T, Naftalovich R and Vatner DE: Healthful aging mediated by inhibition of oxidative stress. Ageing Res Rev 64: 101194, 2020.
10. Sies H and Jones DP: Reactive oxygen species (ROS) as pleiotropic physiological signalling agents. Nat Rev Mol Cell Biol 21: 363-383, 2020.
11. Wang FS, Wu RW, Chen YS, Ko JY, Jahr H and Lian WS: Biophysical modulation of the mitochondrial metabolism and redox in bone homeostasis and osteoporosis: How biophysics converts into bioenergetics. Antioxidants (Basel) 10: 1394, 2021.
12. Khosla S and Hofbauer LC: Osteoporosis treatment: Recent developments and ongoing challenges. Lancet Diabetes Endocrinol 5: 898-907, 2017.
13. Arceo-Mendoza RM and Camacho PM: Postmenopausal osteoporosis: Latest guidelines. Endocrinol Metab Clin North Am 50: 167-178, 2021.
14. Ensrud KE: Bisphosphonates for postmenopausal osteoporosis. JAMA 325: 96, 2021.
15. Buckley L, Guyatt G, Fink HA, Cannon M, Grossman J, Hansen KE, Humphrey MB, Lane NE, Magrey M, Miller M, *et al*: 2017 American college of rheumatology guideline for the prevention and treatment of glucocorticoid-induced osteoporosis. Arthritis Rheumatol 69: 1521-1537, 2017.
16. Reid IR: A broader strategy for osteoporosis interventions. Nat Rev Endocrinol 16: 333-339, 2020.
17. Lv Z and Guo Y: Metformin and its benefits for various diseases. Front Endocrinol (Lausanne) 11: 191, 2020.
18. Foretz M, Guigas B, Bertrand L, Pollak M and Viollet B: Metformin: From mechanisms of action to therapies. Cell Metab 20: 953-966, 2014.
19. Tseng CH: Metformin use is associated with a lower risk of osteoporosis/vertebral fracture in Taiwanese patients with type 2 diabetes mellitus. Eur J Endocrinol 184: 299-310, 2021.
20. Jiating L, Buyun J and Yinchang Z: Role of metformin on osteoblast differentiation in type 2 diabetes. Biomed Res Int 2019: 9203934, 2019.
21. Wang X, Sun Q, Jiang Q, Jiang Y, Zhang Y, Cao J, Lu L, Li C, Wei P, Wang Q and Wang Y: Cryptotanshinone ameliorates doxorubicin-induced cardiotoxicity by targeting Akt-GSK-3β-mPTP pathway in vitro. Molecules 26: 1460, 2021.
22. Yang K, Cao F, Qiu S, Jiang W, Tao L and Zhu Y: Metformin promotes differentiation and attenuates H_2O_2-induced oxidative damage of osteoblasts via the PI3K/AKT/Nrf2/HO-1 pathway. Front Pharmacol 13: 829830, 2022.
23. Yang K, Pei L, Zhou S, Tao L and Zhu Y: Metformin attenuates H_2O_2-induced osteoblast apoptosis by regulating SIRT3 via the PI3K/AKT pathway. Exp Ther Med 22: 1316, 2021.
24. Bai J, Xie N, Hou Y, Chen X, Hu Y, Zhang Y, Meng X, Wang X and Tang C: The enhanced mitochondrial dysfunction by cantleyoside confines inflammatory response and promotes apoptosis of human HFLS-RA cell line via AMPK/Sirt 1/NF-κB pathway activation. Biomed Pharmacother 149: 112847, 2022.
25. Zhang R, Li G, Zhang Q, Tang Q, Huang J, Hu C, Liu Y, Wang Q, Liu W, Gao N and Zhou S: Hirsutine induces mPTP-dependent apoptosis through ROCK1/PTEN/PI3K/GSK3β pathway in human lung cancer cells. Cell Death Dis 9: 598, 2018.
26. Roskoski R Jr: Small molecule inhibitors targeting the EGFR/ErbB family of protein-tyrosine kinases in human cancers. Pharmacol Res 139: 395-411, 2019.
27. Wang S, Zhang Y, Wang Y, Ye P, Li J, Li H, Ding Q and Xia J: Amphiregulin confers regulatory T cell suppressive function and tumor invasion via the EGFR/GSK-3β/Foxp3 axis. J Biol Chem 291: 21085-21095, 2016.
28. Sanchez-Rangel E and Inzucchi SE: Metformin: Clinical use in type 2 diabetes. Diabetologia 60: 1586-1593, 2017.
29. Cameron AR, Morrison VL, Levin D, Mohan M, Forteath C, Beall C, McNeilly AD, Balfour DJ, Savinko T, Wong AK, *et al*: Anti-inflammatory effects of metformin irrespective of diabetes status. Circ Res 119: 652-665, 2016.
30. Yang TC, Duthie GG, Aucott LS and Macdonald HM: Vitamin E homologues α- and γ-tocopherol are not associated with bone turnover markers or bone mineral density in peri-menopausal and post-menopausal women. Osteoporos Int 27: 2281-2290, 2016.
31. Kulkarni AS, Gubbi S and Barzilai N: Benefits of metformin in attenuating the hallmarks of aging. Cell Metab 32: 15-30, 2020.
32. Zhang T, Liu Q, Gao W, Sehgal SA and Wu H: The multifaceted regulation of mitophagy by endogenous metabolites. Autophagy 18: 1216-1239, 2022.
33. Abate M, Festa A, Falco M, Lombardi A, Luce A, Grimaldi A, Zappavigna S, Sperlongano P, Irace C, Caraglia M and Misso G: Mitochondria as playmakers of apoptosis, autophagy and senescence. Semin Cell Dev Biol 98: 139-153, 2020.
34. Panel M, Ghaleb B and Morin D: Mitochondria and aging: A role for the mitochondrial transition pore? Aging Cell 17: e12793, 2018.
35. Wu Y, Yang M, Fan J, Peng Y, Deng L, Ding Y, Yang R, Zhou J, Miao D and Fu Q: Deficiency of osteoblastic Arl6ip5 impaired osteoblast differentiation and enhanced osteoclastogenesis via disturbance of ER calcium homeostasis and induction of ER stress-mediated apoptosis. Cell Death Dis 5: e1464, 2014.
36. Zhu P, Hu S, Jin Q, Li D, Tian F, Toan S, Li Y, Zhou H and Chen Y: Ripk3 promotes ER stress-induced necroptosis in cardiac IR injury: A mechanism involving calcium overload/XO/ROS/mPTP pathway. Redox Biol 16: 157-168, 2018.
37. NavaneethaKrishnan S, Rosales JL and Lee KY: mPTP opening caused by Cdk5 loss is due to increased mitochondrial Ca^{2+} uptake. Oncogene 39: 2797-2806, 2020.
38. Nagini S, Sophia J and Mishra R: Glycogen synthase kinases: Moonlighting proteins with theranostic potential in cancer. Semin Cancer Biol 56: 25-36, 2019.
39. Lal H, Ahmad F, Woodgett J and Force T: The GSK-3 family as therapeutic target for myocardial diseases. Circ Res 116: 138-149, 2015.
40. Morciano G, Naumova N, Koprowski P, Valente S, Sardão VA, Potes Y, Rimessi A, Wieckowski MR and Oliveira PJ: The mitochondrial permeability transition pore: An evolving concept critical for cell life and death. Biol Rev Camb Philos Soc 96: 2489-2521, 2021.
41. Karch J, Bround MJ, Khalil H, Sargent MA, Latchman N, Terada N, Peixoto PM and Molkentin JD: Inhibition of mitochondrial permeability transition by deletion of the ANT family and CypD. Sci Adv 5: eaaw4597, 2019.

42. Wang H, Ai J, Shopit A, Niu M, Ahmed N, Tesfaldet T, Tang Z, Li X, Jamalat Y, Chu P, *et al*: Protection of pancreatic β-cell by phosphocreatine through mitochondrial improvement via the regulation of dual AKT/IRS-1/GSK-3β and STAT3/Cyp-D signaling pathways. Cell Biol Toxicol 38: 531-551, 2022.
43. Hu Z, Crump SM, Zhang P and Abbott GW: Kcne2 deletion attenuates acute post-ischaemia/reperfusion myocardial infarction. Cardiovasc Res 110: 227-237, 2016.
44. Ding L and Billadeau DD: Glycogen synthase kinase-3β: A novel therapeutic target for pancreatic cancer. Expert Opin Ther Targets 24: 417-426, 2020.
45. Kim DH, Triet HM and Ryu SH: Regulation of EGFR activation and signaling by lipids on the plasma membrane. Prog Lipid Res 83: 101115, 2021.
46. Liu G, Xie Y, Su J, Qin H, Wu H, Li K, Yu B and Zhang X: The role of EGFR signaling in age-related osteoporosis in mouse cortical bone. FASEB J 33: 11137-11147, 2019.
47. Phukan S, Babu VS, Kannoji A, Hariharan R and Balaji VN: GSK3beta: Role in therapeutic landscape and development of modulators. Br J Pharmacol 160: 1-19, 2010.
48. Zhang Z, Lv Z, Zhang W, Guo M and Li C: A novel β-catenin from Apostichopus japonicus mediates Vibrio splendidus-induced inflammatory-like response. Int J Biol Macromol 156: 730-739, 2020.